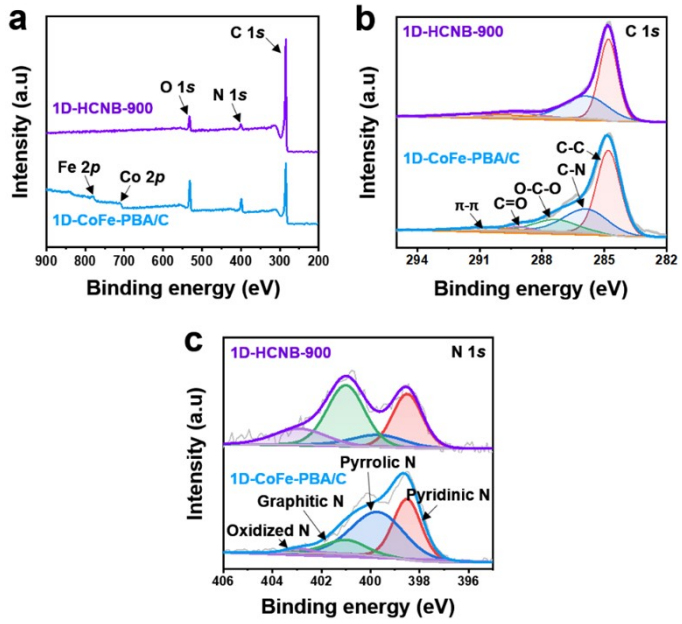

Figure S1. (a) Survey X-ray photoelectron spectroscopy (XPS) spectra of 1D-CoFe-PBA/C and 1D-HCNB-900. (b) High-resolution XPS spectra for (b) C 1*s* and (c) N 1*s* of 1D-CoFe-PBA/C and 1D-HCNB-900.

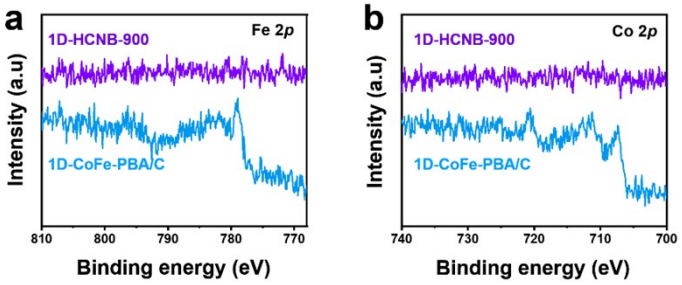

Figure S2. High-resolution XPS (HRXPS) spectra for (a) Fe 2*p* and (b) Co 2*p* of 1D-CoFe-PBA/C and 1D-HCNB-900.

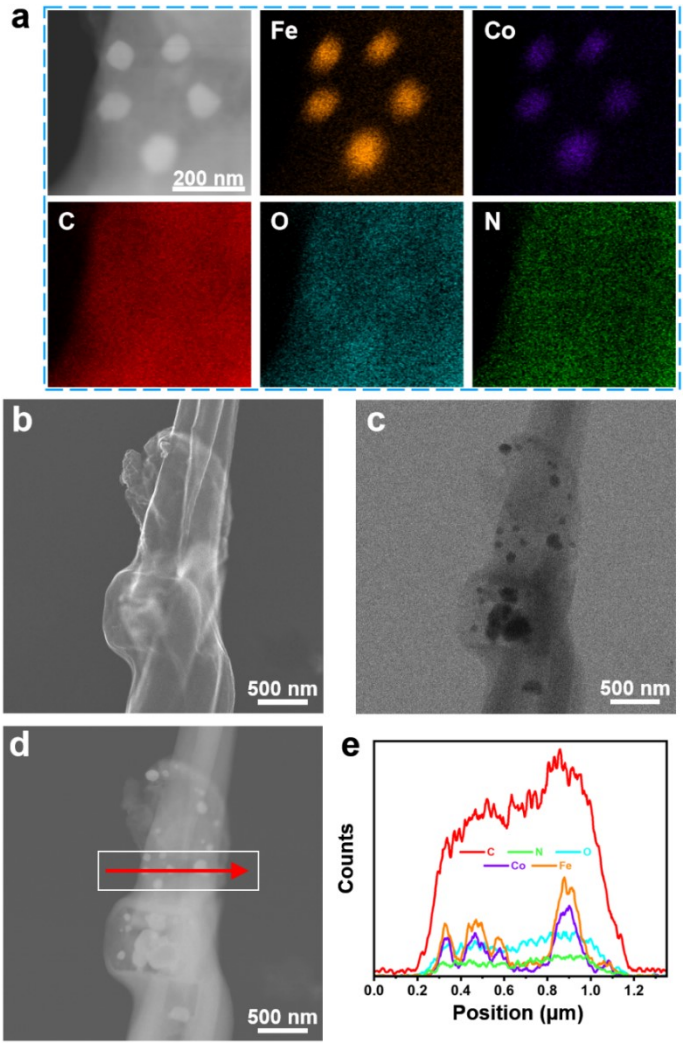

Figure S3. (a) Scanning transmission electron microscopy (STEM) elemental mapping of 1D-CoFe-PBA/C. (b) Secondary electron, (c) bright-field, and (d) dark-field STEM images of 1D-CoFe-PBA/C. (e) STEM elemental line scan profile of 1D-CoFe-PBA/C.

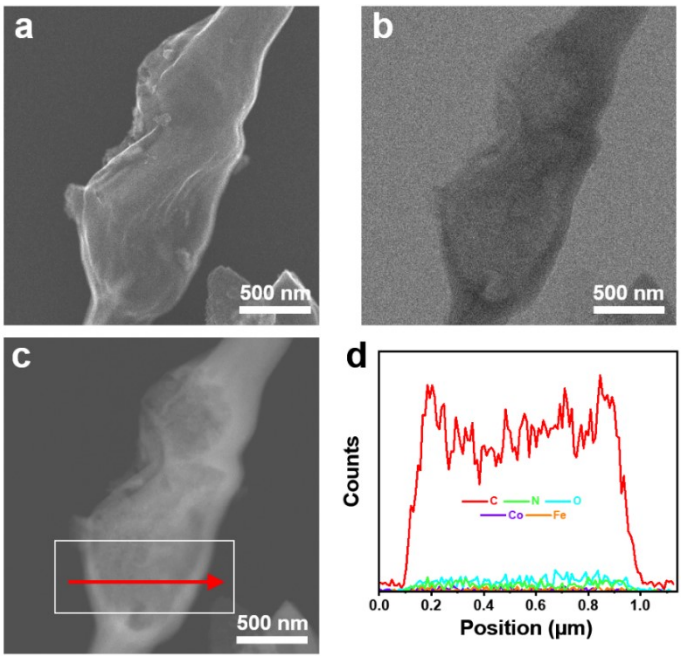

Figure S4. (a) Secondary electron, (b) bright-field, and (c) dark-field STEM images of 1D-HCNB-900. STEM elemental line scan profile of 1D-HCNB-900.

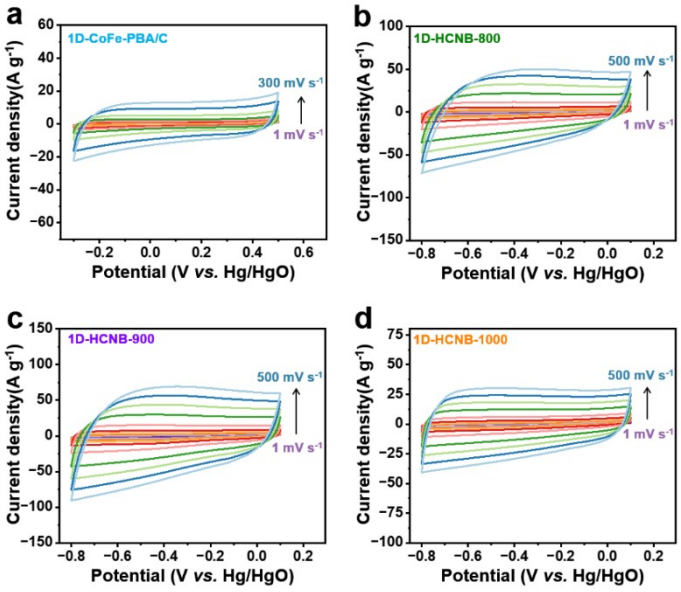

Figure S5. CV curves of (a) 1D-CoFe-PBA/C, (b) 1D-HCNB-800, (c) 1D-HCNB-900, and (d) 1D-HCNB-1000 over a range of scan rates.

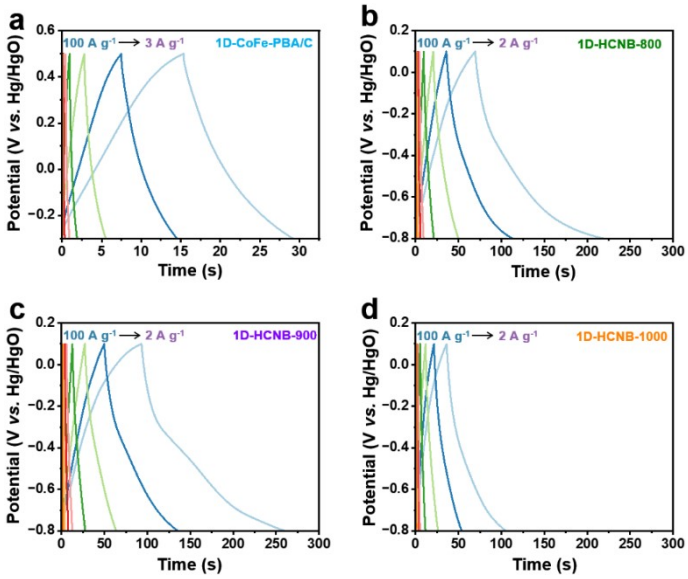

Figure S6. GCD curves of (a) 1D-CoFe-PBA/C, (b) 1D-HCNB-800, (c) 1D-HCNB-900, and (d) 1D-HCNB-1000 over a range of current densities.

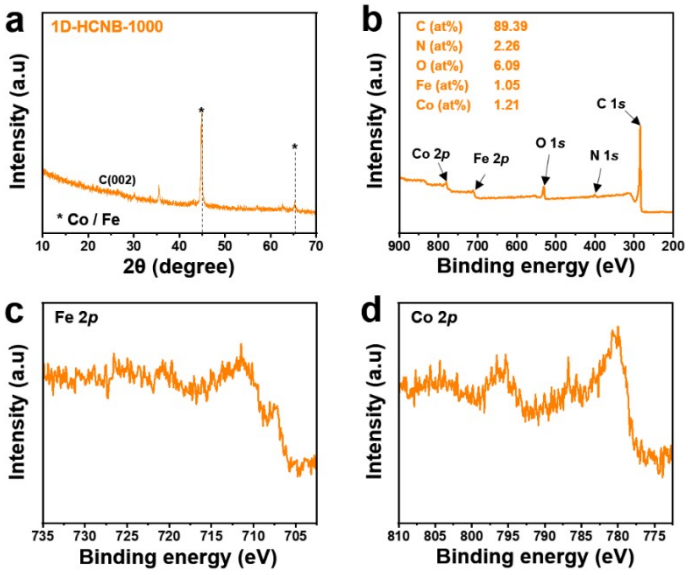

Figure S7. (a) XRD and (b) survey XPS spectra of 1D-HCNB-1000. (c) HRXPS spectra for (c) Fe 2*p* and (d) Co 2*p* of 1D-HCNB-1000.

Note: The appearance of Co 2*p* and Fe 2*p* peaks in XPS spectra of 1D-HCNB-1000 (**Fig. S7b-d**) is potentially due to the agglomeration of Co and Fe atoms to metallic nanoparticles after calcination at such high temperature of 1000 °C. When Co and Fe atoms are present in the form of nanoparticles,

they are easily detected by XPS. On the contrary, the two peaks are not detected in the XPS spectra of 1D-HCNB-900 because Fe and Co atoms exist in the form of very small nanoclusters, which are often not easily detected by XPS (**Fig. S2a**, **b**).

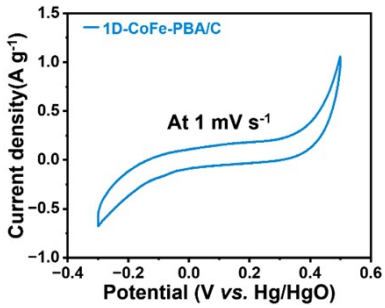

Figure S8. CV curve of 1D-CoFe-PBA/C at 1 mV s^{-1}.

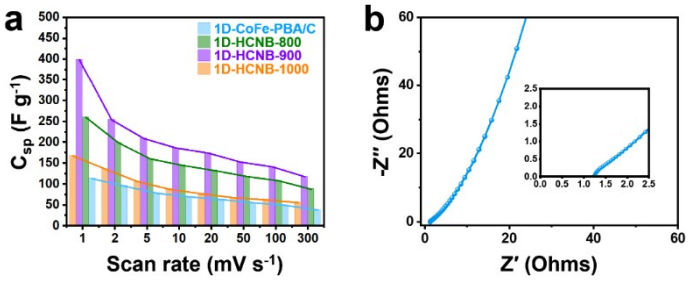

Figure S9. (a) Capacitance retention rate of 1D-CoFe-PBA/C and 1D-HCNBs over a range of scan rates (1 to 300 mV s^{-1}) and (b) Nyquist plot of 1D-CoFe-PBA/C.

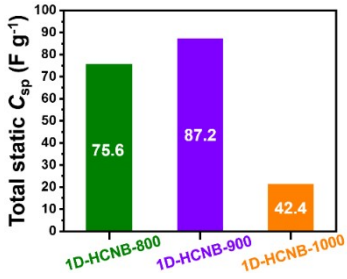

Figure S10. Complex capacitance of 1D-HCNB-900, 1D-HCNB-900 and 1D-HCNB-1000.

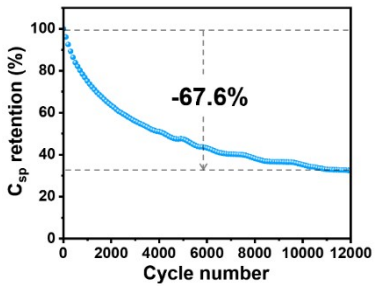

Figure S11. Percentage of capacitance retention of 1D-CoFe-PBA/C over 12000 cycles at 10 A g^{-1}.

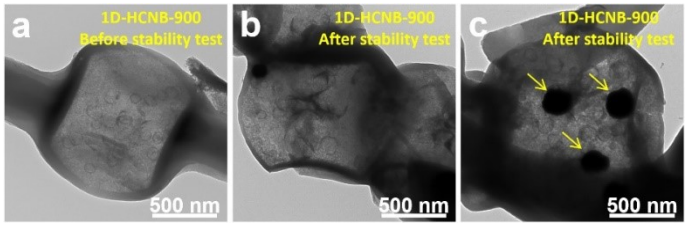

Figure S12. TEM images of 1D-HCNB-900 (a) before and (b, c) after the stability test with 15000 consecutive GCD cycles.

Table S1. Atomic percentage (at%) of C, N, O, Co, and Fe calculated from the survey XPS spectra of 1D-CoFe-PBA/C and 1D-HCNB-900.

	C (at%)	N (at%)	O (at%)	Co (at%)	Fe (at%)
1D-CoFe-PBA/C	73.55	11.14	13.32	1.08	0.91
1D-HCNB-900	91.18	4.62	4.20	0.00	0.00

Table S2. Specific surface area (S_{BET}) calculated by BET method and pore volume calculated from NLDFT method from nitrogen adsorption/desorption isotherms.

	S_{BET} (m^2 g^{-1})	Pore Volume (cm^3 g^{-1} nm^{-1})
1D-HCNB-800	282.7	0.326
1D-HCNB-900	457.6	0.279
1D-HCNB-1000	366.3	0.419

Table S3. Specific capacitance of 1D-CoFe-PBA/C and 1D-HCNB-*x* (where *x*= 800 or 900 or 1000) obtained from GCD curves at various current densities.

	Current densities (A g^{-1})							
	2	3	5	10	20	30	50	100
1D-CoFe-PBA/C	80.8	66.6	51.7	55.5	47.6	-	-	-
1D-HCNB-800	332.2	256.1	164.0	129.6	108.9	98.0	83.8	58.7
1D-HCNB-900	370.0	288.2	200.6	165.5	146.4	134.0	128.5	112.2
1D-HCNB-1000	153.4	107.5	80.3	67.5	59.7	55.9	50.9	42.0

Table S4. Specific capacitance of 1D-CoFe-PBA/C and 1D-HCNB-*x* (where *x*= 800 or 900 or 1000) obtained from CV curves at various scan rates.

	Scan rates (mV s^{-1})								
	1	5	10	20	50	100	200	400	500
1D-CoFe-PBA/C	112.5	77.8	69.3	62.7	55.0	48.8	42.0	-	-
1D-HCNB-800	259.6	160.0	144.4	132.0	117.9	107.5	94.5	80.5	73.5
1D-HCNB-900	398.5	208.9	186.1	173.9	152.4	140.8	127.1	109.5	103.1
1D-HCNB-1000	167.3	105.9	87.3	76.3	67.0	62.1	57.9	53.1	51.4

Table S5. Summary of porous carbon electrode materials for supercapacitors.

Carbon type	Electrolyte	Current density (A g^{-1})	Specific capacitance (F g^{-1})	Ref.
CoHCF hollow prism	0.5 M Na_2SO_4	2.0	258.6	1
CoHCF/rGO (20 wt%)	0.5 M Na_2SO_4	1.0	340.0	2
CN-Co/0.05S	6 M KOH	1.0	334.0	3
CoHCF submicroboxes	0.5 M Na_2SO_4	0.5	288.0	4
CMC-2	6 M KOH	1.0	353.0	5
CoHCF	0.5 M Na_2SO_4	1.0	250.0	6
PB-Co (0.3)/rGOH	1 M KNO_3	1.0	220.0	7
HCP-pXy-800	3 M KOH	1.25	242.5	8
CPC1_700	6 M KOH	1.0	270.0	9
B-AC	2 M KOH	1.0	330.0	10
1D-HCNB-900	**2 M KOH**	**2.0**	**370.0**	**This work**

References

1. X. Yin, H. Li, H. Wang, Z. Zhang, R. Yuan, J. Lu, Q. Song, J.-G. Wang, L. Zhang and Q. Fu, *ACS Appl. Mater. Interfaces*, 2018, **10**, 29496-29504.
2. J.-G. Wang, Z. Zhang, X. Liu and B. Wei, *Electrochim. Acta*, 2017, **235**, 114-121.
3. J.-s. Gao, Z. Zhang, H. Wang, Z. Liu and Y. He, *J. Electroanal. Chem.*, 2022, **921**, 116670.
4. J.-G. Wang, Z. Zhang, X. Zhang, X. Yin, X. Li, X. Liu, F. Kang and B. Wei, *Nano Energy*, 2017, **39**, 647-653.
5. Y. Boyjoo, Y. Cheng, H. Zhong, H. Tian, J. Pan, V. K. Pareek, S. P. Jiang, J.-F. Lamonier, M. Jaroniec and J. Liu, *Carbon*, 2017, **116**, 490-499.
6. F. Zhao, Y. Wang, X. Xu, Y. Liu, R. Song, G. Lu and Y. Li, *ACS Appl. Mater. Interfaces*, 2014, **6**, 11007-11012.
7. X. Zhang, J. Jiang, Y. Chen, K. Cheng, F. Yang, J. Yan, K. Zhu, K. Ye, G. Wang, L. Zhou and D. Cao, *Chem. Eng. J.*, 2018, **335**, 321-329.
8. S.-H. Kim, R. Vinodh, C. V. V. M. Gopi, V. G. R. Kummara, S. Sambasivam, I. M. Obaidat and H.-J. Kim, *Mater. Lett.*, 2020, **263**, 127222.
9. Y. K. Kim, J. H. Park and J. W. Lee, *Carbon*, 2018, **126**, 215-224.
10. C. Peng, X.-b. Yan, R.-t. Wang, J.-w. Lang, Y.-j. Ou and Q.-j. Xue, *Electrochim. Acta*, 2013, **87**, 401-408.